

1                    **Comprehensive antibody profiling of mRNA vaccination in children**

2    **Authors:** Yannic C Bartsch, PhD <sup>1</sup>; Kerri J St Denis<sup>1</sup>; Paulina Kaplonek, PhD ; Jaewon Kang<sup>1</sup>;  
3    Evan C. Lam<sup>1</sup>; Madeleine D Burns<sup>2</sup>; Eva J Farkas<sup>2</sup>; Jameson P Davis<sup>2</sup>; Brittany P Boribong, PhD  
4    <sup>2</sup>; Andrea G Edlow, MD<sup>3</sup>; Alessio Fasano, MD<sup>2</sup>; Wayne Shreffler, MD PhD<sup>4</sup>; Dace Zavadska, MD  
5    PhD<sup>5</sup>; Marina Johnson, PhD<sup>6</sup>; David Goldblatt, PhD<sup>6</sup>; Alejandro B Balazs, PhD<sup>1</sup>; Lael M Yonker,  
6    MD<sup>2#</sup>; Galit Alter, PhD <sup>1#</sup>

7    **Affiliations:**

8    <sup>1</sup> Ragon Institute of MGH, MIT, and Harvard, Cambridge, MA, USA

9    <sup>2</sup> Massachusetts General Hospital Department of Pediatrics, Mucosal Immunology and Biology  
10    Research Center, Boston, MA, USA

11    <sup>3</sup> Massachusetts General Hospital Department of Obstetrics and Gynecology, Division of  
12    Maternal-Fetal Medicine, Vincent Center for Reproductive Biology, Boston, MA, USA

13    <sup>4</sup> Massachusetts General Hospital Food Allergy Center, Division of Pediatric Allergy and  
14    Immunology, Boston, MA, USA

15    <sup>5</sup> Children's Clinical University Hospital, Riga, Latvia

16    <sup>6</sup> Great Ormond Street Institute of Child Health Biomedical Research Centre, University College  
17    London, London, UK

18

19    \*correspondence: [LYONKER@mgh.harvard.edu](mailto:LYONKER@mgh.harvard.edu) and [GALTER@mgh.harvard.edu](mailto:GALTER@mgh.harvard.edu)

20

21 **Abstract:** While children have been largely spared from COVID-19 disease, the emergence of  
22 viral variants of concern (VOC) with increased transmissibility, combined with fluctuating mask  
23 mandates and school re-openings have led to increased infections and disease among children.  
24 Thus, there is an urgent need to roll out COVID-19 vaccines to children of all ages. However,  
25 whether children respond equivalently to adults to mRNA vaccines and whether dosing will elicit  
26 optimal immunity remains unclear. Given the recent announcement of incomplete immunity  
27 induced by the pediatric dose of the BNT162b2 vaccine in young children, here we aimed to deeply  
28 profile and compare the vaccine-induced humoral immune response in 6-11 year old children  
29 receiving the pediatric (50 $\mu$ g) or adult (100 $\mu$ g) dose of the mRNA-1273 vaccine compared to  
30 adults and naturally infected children or children that experienced multi inflammatory syndrome  
31 in children (MIS-C) for the first time. Children elicited an IgG dominant vaccine induced immune  
32 response, surpassing adults at a matched 100 $\mu$ g dose, but more variable immunity at a 50 $\mu$ g dose.  
33 Irrespective of titer, children generated antibodies with enhanced Fc-receptor binding capacity.  
34 Moreover, like adults, children generated cross-VOC humoral immunity, marked by a decline of  
35 omicron receptor binding domain-binding, but robustly preserved omicron Spike-receptor binding,  
36 with robustly preserved Fc-receptor binding capabilities, in a dose dependent manner. These data  
37 indicate that while both 50 $\mu$ g and 100 $\mu$ g of mRNA vaccination in children elicits robust cross-  
38 VOC antibody responses, 100 $\mu$ g of mRNA in children results in highly preserved omicron-specific  
39 functional humoral immunity.

40 **One-Sentence Summary:** mRNA vaccination elicits robust humoral immune responses to SARS-  
41 CoV-2 in children 6-11 years of age.

## 42 **Introduction**

43 The burden of respiratory infections is often higher in young children with a developing untrained  
44 immune system(1). However, lower rates of disease were noted early in the COVID-19 pandemic  
45 among children, who largely experienced asymptomatic or pauci-symptomatic SARS-CoV-2  
46 infections(2). However, with the rise of highly infectious variants of concern (VOCs), like the  
47 novel omicron VOC, increasing infection rates and hospitalizations have been observed globally(3,  
48 4). Linked to the unpredictable incidence of multisystem inflammatory syndrome in children  
49 (MIS-C) and the clear contribution children make to population level spread, the need for vaccines  
50 for children is evident (5, 6). However, whether newly emerging COVID-19 vaccine platforms,  
51 approved for teenager/adult use, elicit immunity in children is not well understood.

52 Epidemiologic data clearly highlight vulnerabilities in the pediatric immune system, with  
53 increased rates of respiratory, enteric, and parasitic infections disproportionately causing disease  
54 in children in the first decade of life(7, 8). In fact, vaccine-induced immune responses often differ  
55 across children and adults(9). However, whether these vulnerabilities to infection and poor  
56 response to protein-based vaccination will translate to newer vaccine platforms, like mRNA  
57 vaccine platforms, remains unclear. Moreover, emerging data suggests that dosing may not be  
58 straight forward for mRNA vaccines (10, 11), due to reduced immunogenicity in young children,  
59 requiring deeper immunologic insights to guide rational pediatric vaccine design.

60 To begin to define the humoral mRNA vaccine responses in children, we comprehensively profiled  
61 vaccine-induced immune responses in children (6-11 years) who received the pediatric (50µg) or  
62 adult (100µg) dose of the mRNA-1273 vaccine regimen, respectively. We observed 100% vaccine  
63 response rates prior to the second vaccine dose in children that received the 100µg vaccine dose.  
64 While immune profiles in the low (50µg) dose were more similar to adults (who received the adults

65 recommended 100 $\mu$ g dose), children receiving the adult (100 $\mu$ g) dose generated disproportionately  
66 higher IgG biased vaccine responses following the second vaccine dose, with enhanced Fc-effector  
67 profiles. Moreover, both pediatric and adult doses elicited broad cross-variant isotype and Fc-  
68 receptor binding antibodies, however, while all groups experienced a significant loss of omicron-  
69 receptor binding domain (RBD) reactivity, omicron Spike-specific immunity was largely  
70 preserved and 100 $\mu$ g immunized children exhibited the highest cross-reactivity. Collectively, these  
71 data point to robust, but dose dependent, functional humoral pediatric immune signatures induced  
72 in children following mRNA-1273 vaccination.

### 73 **Results**

74 In the wake of fluctuating mask mandates, school re-openings, and the rapid spread of the highly  
75 infectious SARS-CoV-2 delta and omicron variants, a surge of SARS-CoV-2 infections in children  
76 has been observed (5). Increasing numbers of children with severe COVID-19 or life-threatening  
77 Multisystem Inflammatory Syndrome in Children (MIS-C), plus our evolving appreciation of  
78 children in the spread of the pandemic, there is an urgent need to roll out vaccines across all ages.  
79 With the rapid roll out of mRNA vaccines, it remains unclear whether children will generate  
80 sufficiently robust immunity following mRNA vaccination. Here we deeply characterized the  
81 immune response induced by the Moderna mRNA-1273 vaccine in children that received an adult  
82 dose (100 $\mu$ g) of mRNA-1273 (n=12; median age= 9 years range: 7 – 11 years; 42% female),  
83 matching the recommendations for adults, or a pediatric (50 $\mu$ g) dose of mRNA-1273 (n=12;  
84 median age= 8 years range: 5 – 11 years; 50% female) at days 0 and 28, respectively. Plasma  
85 samples were collected before vaccination (V0), approximately four weeks after prime (V1) and  
86 four weeks after second (V2) immunization.

87 *mRNA vaccines induce robust SARS-CoV-2 spike binding and neutralizing titers in children*

88 To begin to investigate the vaccine-induced humoral response, we profiled SARS-CoV-2 Spike  
89 (S) specific antibody titers. At V1, we observed seroconversion (marked by an increase in Spike  
90 specific IgM, IgA1 or IgG1 binding compared to V0) in 100 % of children receiving the 50 $\mu$ g  
91 (n=9/9) or 100 $\mu$ g (n=12/12) dose of mRNA-1273. Both S-specific IgA1 and IgG1 increased with  
92 the second dose, while S-specific IgM responses declined slightly, marking efficient class  
93 switching. After the second dose we observed significantly elevated S-specific IgA1 levels in  
94 adults compared to children (p-value: <0.001) (**Figure 1A**). In contrast, children in the 100 $\mu$ g dose  
95 group elicited higher IgG1 titers after the first and second dose of the vaccine compared to children  
96 in the 50 $\mu$ g dose group (p-value: 0.004), as well as compared to vaccinated adults (p-value: 0.03).  
97 Likewise, we observed a trend towards higher neutralizing antibody titers in the pediatric 100 $\mu$ g  
98 dose group followed by adults and 50 $\mu$ g vaccinated children (**Figure 1B**). Univariate comparison  
99 of V2 levels of the 100 $\mu$ g adults to 100 $\mu$ g and 50 $\mu$ g children highlighted isotype selection  
100 differences across children and adults, but minimal overall differences in antibody binding titers  
101 and neutralization across the 50 and 100 $\mu$ g doses in children (**Figure 1C**). Furthermore, vaccine-  
102 induced binding and neutralization titers in the 100 $\mu$ g pediatric dose group were higher compared  
103 to levels observed in naturally exposed convalescent children or MIS-C. Importantly, while these  
104 differences may be related to exposure to different variants, we observed superior vaccine induced  
105 binding and neutralization to all variants, highlighting the critical importance of SARS-CoV-2  
106 vaccination in promoting broader VOC immunity in children compared to infection  
107 (**Supplemental Figure 1 and 2**). Taken together, these data show that mRNA vaccination can  
108 elicit strong but dose-dependent anti-SARS-CoV-2 binding and neutralizing titers in children  
109 superior to natural infection that are accompanied by some age-dependent shifts in isotype-  
110 antibody profiles.

111 *mRNA vaccination induces highly potent Spike-specific Fc effector functions in children*

112 In addition to binding and neutralization, protection against severe adult COVID-19 has been  
113 linked to the ability of antibodies to leverage additional antiviral functions via Fc-receptors to fight  
114 infection, referred to as antibody effector functions(12-14). Specifically, opsonophagocytic  
115 pathogen clearance is key to protection against several bacterial pathogens and cytotoxic antibody  
116 functions have been linked to protection against viruses(15, 16). Thus, we profiled the relative  
117 ability of vaccine-induced immune responses to bind to human Fc-receptors (Fc $\gamma$ R2a, Fc $\gamma$ R2b,  
118 Fc $\gamma$ R3a, Fc $\gamma$ R3b, and Fc $\alpha$ R) as well as their ability to elicit antibody-dependent complement  
119 deposition (ADCD), antibody dependent neutrophil phagocytosis (ADNP), antibody dependent  
120 monocyte phagocytosis (ADCP), or activation antibody dependent NK cell activation (ADNKA).  
121 Children in both dose groups elicited Spike (S)-specific IgG antibodies that bound robustly to all  
122 Fc-receptors following the first dose, markedly greater than responses observed in vaccinated  
123 adults and in natural COVID-19 infection or MIS-C (**Figure 2A**). Moreover, these responses  
124 expanded further after the second immunization with significantly elevated antibody-Fc-receptor  
125 binding in the 100 $\mu$ g pediatric dose group compared to the 50 $\mu$ g dose, with significant higher  
126 Fc $\gamma$ R3a and slightly higher Fc $\gamma$ R2a, Fc $\gamma$ R2b and Fc $\gamma$ R3b binding compared to the 100 $\mu$ g adult  
127 group (**Figure 2B**). Interestingly, this increased Fc-receptor binding was not directly related to  
128 overall changes in Spike-specific IgG subclass selection (**Supplemental Figure 1**), pointing to  
129 alternate mechanisms for augmented humoral immune function in children, potentially linked to  
130 pediatric selection of more potent Fc-glycosylation profiles(17). In contrast, compared to adults,  
131 children induced lower levels of IgA antibodies that exhibited, as expected, lower interactions with  
132 the IgA-Fc-receptor, Fc $\alpha$ R, compared to adults (**Figure 2B and Supplemental Figure 2**)(18, 19).

133 To next determine whether these distinct pediatric Fc $\gamma$ -receptor binding profiles translated to more  
134 functional Spike-specific humoral immune responses, we examined vaccine-induced Fc-effector  
135 functions (**Figure 2C**). Interestingly, low levels of ADCD, ADNP and ADCP were observed after  
136 primary immunization, but were notably augmented by the second immunization across the  
137 groups, resulting in significantly increased ADCD and ADNP in the 100 $\mu$ g vaccinated children  
138 compared to adults or the 50 $\mu$ g pediatric dose (**Figure 2C**). In contrast, NK cell functions (as  
139 measured by MIP-1b expression) were induced to equal levels across all groups. Overall, high  
140 dose mRNA-1273 induced higher levels of ADCD, ADNP and ADCP recruiting antibodies in  
141 children compared to adults following the 100 $\mu$ g vaccine regimen (**Figure 2D**). These data point  
142 to enhanced functional antibody responsiveness in children at a matched 100 $\mu$ g dose compared to  
143 adults, and a solid functional response at the optimized 50 $\mu$ g dose endowing children with a robust  
144 capacity to recruit immune function at half the adult dose, all higher than levels observed following  
145 natural infection or MIS-C.

#### 146 *Selective expansion of opsonophagocytic antibodies with mRNA vaccination in children*

147 To gain a more granular sense of the differences in immune responses across children and adults  
148 at the same matched dose or across children receiving the 50 and 100 $\mu$ g doses, we next utilized a  
149 machine learning approach to probe the humoral immune features that differed most across these  
150 groups. As few as six of the overall features analyzed across all plasma samples, were sufficient  
151 to completely resolve vaccine induced immune responses induced by the 100 $\mu$ g dose across  
152 children and adults (**Figure 3A+B**). Specifically, vaccine-induced S-specific IgG1, Fc $\gamma$ R3a  
153 binding, ADNP and ADCD were all enriched selectively in children, whereas Spike-specific IgM  
154 and IgA1 titers were enriched in adults (**Figure 3A**), highlighting distinct isotype selection in  
155 adults, and the generation of more functional antibodies in children. Conversely, comparison of

156 50 and 100 $\mu$ g doses in children was achieved using only two of all antibody features analyzed  
157 for each plasma. These features Spike-specific ADNP and IgG4 levels, both of which were  
158 enriched in the immune profiles in children that received the 100 $\mu$ g dose of the vaccine (**Figure**  
159 **3C+D**). Additionally, in contrast to natural infection, vaccination induced higher titers and  
160 functions to SARS-CoV-2 when comparing vaccinated children to those that were previously  
161 infected (**Figure 2 and Supplemental Figure 3**). Collectively, these data point to slight shifts in  
162 isotype selection between adults and children, but the potential for children to raise more  
163 functional antibodies, that match those of adults at a half-dose.

164 *mRNA vaccination in children raises robust responses against SARS-CoV-2 variants of concern*

165 Real-world efficacy suggests that mRNA vaccines confer robust protection against severe  
166 disease/death against the original (wildtype; wt) SARS-CoV-2 strain (Wuhan), at levels greater  
167 than 90% (20). This level of efficacy appears to be sustained against evolving variants of concern  
168 (VOCs), including the alpha and delta variants, although lower levels of protection have been  
169 observed against the beta variant (21, 22). While previous VOCs were marked by single or few  
170 amino acid substitutions, the novel omicron variant has 29 mutations in the Spike protein, resulting  
171 in enhanced transmissibility, and a concomitant loss of neutralizing titers (23, 24). Yet, despite the  
172 striking increase in omicron transmissibility, a similar increase in severe disease and death has not  
173 been observed, suggesting that alternate vaccine induced immune responses may continue to afford  
174 protection against severe disease and death. To explore whether mRNA vaccination in children  
175 results in the generation of vaccines with differential VOC recognition capabilities (25). We  
176 observed a progressive loss of IgM, IgA, and IgG binding to VOC RBDs across both pediatric  
177 groups and adults, with more variable cross-VOC IgG responses among 50 $\mu$ g immunized children,  
178 but a consistent and significant loss of binding to the omicron RBD across all 3 groups (Figure



179 4A). Conversely, Spike-specific responses were more resilient across most VOCs, across the 3  
180 groups, except for omicron-Spike-specific responses that were significantly lower across IgM and  
181 IgA response across the groups (Figure 4B). Yet, IgG responses showed 3 different patterns: 1)  
182 50 $\mu$ g immunized children experienced heterogeneous responses across VOCs, marked by some of  
183 the lowest omicron-responses, 2) adults exhibited more stable Spike VOC-IgG binding levels, but  
184 experienced a significant reduction in omicron-Spike reactivity, and 3) 100 $\mu$ g immunized children  
185 exhibited negligible reduction in Spike-specific recognition across VOCs, including to the omicron  
186 Spike. Furthermore, Fc-receptor binding capability was largely preserved across RBD VOCs,  
187 except for omicron RBD-binding which was significantly lower across all 3 groups (Figure 4C).  
188 However, Spike-VOC binding differed across the 3 groups. While wildtype, alpha, beta, and delta  
189 VOC Fc-receptor binding profiles were highly preserved across all 3 groups, omicron-Spike Fc-  
190 receptor binding was most significantly lost in 50 $\mu$ g immunized children (Figure 4D). Adults  
191 exhibited an intermediate loss of omicron-Spike Fc-receptor binding, with a more pronounced  
192 preservation of the opsinophagocytic Fc $\gamma$ R2a and cytotoxic Fc $\gamma$ R3a binding. Conversely, 100 $\mu$ g  
193 immunized children exhibited a negligible loss of Fc-receptor binding to the omicron Spike,  
194 pointing to the generation of highly resilient antibodies in children at the adult dose that continue  
195 to bind to the omicron Spike despite the significant loss of RBD binding. Whether children  
196 generate broader or more flexible humoral immune response at the 100 $\mu$ g dose, enabling them to  
197 preserve immunity to VOCs remains unclear, but the data point to dose and age dependent effects  
198 of antibody-mediated cross-VOC recognition. Whether differences in neutralization and Fc-  
199 function lead to differences in disease-breakthrough across the ages remains unclear but provides  
200 some additional immunological insights that may continue to explain the epidemiologic  
201 differences in disease severity globally in the setting of emerging VOCs.

202

203 **Discussion**

204 mRNA vaccine platforms responded rapidly to SARS-CoV-2 threat, demonstrating robust levels  
205 of efficacy in adults(26, 27). However, despite the successes of SARS-CoV-2 vaccines, the global  
206 roll out has begun to highlight key vulnerable populations, and strategic gaps, that may limit the  
207 impact of vaccination globally. Although children generally experience mild symptoms, they can  
208 harbor robust, high levels of SARS-CoV-2 replication, thereby contributing significantly to viral  
209 spread(28-30). Furthermore, increasing numbers of children are suffering from severe COVID-19  
210 with over 28,000 hospitalizations and over 700 deaths in the US alone as of December 2021 (31).  
211 However, because children have a more naïve immune system that evolves with age it was  
212 uncertain how the mRNA vaccine platforms would impact immunogenicity in young children.  
213 Additionally, recent results suggest that dose adjustments for very young children, due to safety  
214 and tolerance concerns, have introduced additional variation in immunogenicity, resulting in poor  
215 immunogenicity in children under 5 years, who received a lower dose than the adult recommended  
216 30µg dose (11). Thus, in the absence of empirical data, optimal dosing is uncertain. Thus, here we  
217 aimed to dive deeply in defining humoral profile differences across doses and across children and  
218 adults. Similar to results with the Pfizer and Moderna mRNA vaccine trials in teenagers (32, 33),  
219 here we found that the Moderna mRNA vaccine was highly immunogenic in 6-11 year old  
220 children, generating a humoral response superior to that seen following viral exposure. However,  
221 granular vaccine-induced humoral profiling identified significant differences in adult and pediatric  
222 vaccine responses, marked by a selective induction of highly functional IgG responses, with fewer  
223 IgA and IgM responses compared to adults. At a matched 100µg dose, children mounted more

224 robust opsonophagocytic functions, and Fc $\gamma$ -receptor binding compared to adults. Moreover, at  
225 half the adult dose, children mounted equal, albeit more variable, responses compared to adults.

226 Virus neutralization represents a key surrogate marker of vaccine protection against COVID-19.  
227 Yet despite the loss of neutralization against several emerging variants of concern (VOCs), mRNA  
228 vaccines continue to provide protection against severe disease and death(21, 34). Interestingly,  
229 opsonophagocytic functions of antibodies, rather than neutralization alone, have been linked to  
230 survival of COVID-19 following natural infection(12) and are associated with protection from  
231 infection in animal models(35, 36). Here, when immunized with the adult dose, children induced  
232 comparable neutralization but exhibited a preferential expansion of opsonophagocytic functions  
233 compared to adults. The enhanced opsonophagocytic function was not linked to differential  
234 subclass or isotype selection, suggesting that children may induce more functional antibodies via  
235 alternate changes to the humoral immune response, including potential differences in post-  
236 translational IgG modification that may lead to more flexible, highly functional responses,  
237 representing an evolutionary adaptation enabling children to react more flexibly to infections(37).

238 The adaptive immune response matures during the first decade of life(38). Several lines of  
239 evidence suggest that the more naïve immune response in children may allow the immune system  
240 to adapt and evolve more easily to new pathogens, poised to generate broader immunity to new  
241 viruses(39, 40). Moreover, throughout life, our naïve clonal repertoire or immune cells shift in  
242 response to the sequence of pathogens and vaccines we are exposed to. Thus, naïve children may  
243 have a less “biased” repertoire, enabling the generation of immunity to a broader range of  
244 pathogens(41). Along these lines, we observed robust induction of immunity against most VOCs,  
245 with the exception of omicron. However, IgG and Fc-receptor binding profiles were highly similar  
246 among children and adults, although 100 $\mu$ g immunized children induced IgG that were more

247 resilient against VOCs, exhibiting robust recognition of the omicron Spike, whereas both 50 $\mu$ g  
248 immunized children and 100 $\mu$ g immunized adults both lost partial recognition of the omicron  
249 Spike. These data suggest that higher pediatric dosing can result in more flexible humoral  
250 immunity in children against highly divergent VOCs, superior to those induced in adults at a  
251 matched dose. Thus, children may generate more functional Fc-effector functions, that while not  
252 neutralizing, may be poised for rapid elimination of the pathogen upon transmission, providing a  
253 highly effective means to prevent COVID-19.

254 With the increasing spread of SARS-CoV-2 omicron among younger populations (42), increasing  
255 incidence of COVID-19 among the pediatric population, the rare incidence of MIS-C, and the  
256 recent appreciation for long-COVID in children, the need to determine whether SARS-CoV-2  
257 vaccines can elicit functional immune responses will be key to protect children(3, 5, 28, 43, 44).  
258 Comparable to previous observations in adults(10), the mRNA-1273 vaccine induced robust  
259 binding titers, neutralization, and Fc effector function in vaccinated children, in a dose dependent  
260 manner, compared to children diagnosed with COVID-19 or MIS-C, pointing to the importance of  
261 vaccination to robustly bolster immunity to SARS-CoV-2 and emerging VOCs to provide broader  
262 and more potent immunity to SARS-CoV-2. Whether these responses will wane differentially  
263 across doses, whether they will be more protective against particular VOCs, and whether children  
264 will require boosting remains unclear, however, these findings support vaccination of children with  
265 mRNA-1273 as a safe and effective strategy to protect children against COVID-19, MIS-C, and  
266 Long-COVID.

## 267 **Contributions**

268 Y.C.B. and J.K. performed the serological experiments. K.J.D, E.C.L and A.B.B. performed the  
269 neutralization assay. Y.C.B., L.M.Y. and G.A. analyzed and interpreted the data. M.D.B., E.J.F.,

270 J.P.D., B.P.B., A.G.F., A.F., W.S., D.Z., M.J., D.G., and L.M.Y. supervised and managed the  
271 sample collection. G.A. supervised the project. Y.C.B., L.M.Y. and G.A. drafted the manuscript.  
272 All authors critically reviewed the manuscript.

273

## 274 **Acknowledgment**

275 We thank Nancy Zimmerman, Mark and Lisa Schwartz, an anonymous donor (financial support),  
276 Terry and Susan Ragon, and the SAMANA Kay MGH Research Scholars award for their support.  
277 We acknowledge support from the Ragon Institute of MGH, MIT, and Harvard, the Massachusetts  
278 Consortium on Pathogen Readiness (MassCPR), the NIH (3R37AI080289-11S1, R01AI146785,  
279 U19AI42790-01, U19AI135995-02, U19AI42790-01, 1U01CA260476 – 01,  
280 CIVIC75N93019C00052, 5K08HL143183), the Gates Foundation Global Health Vaccine  
281 Accelerator Platform funding (OPP1146996 and INV-001650), and the Musk Foundation.

## 282 **Competing interests**

283 G.A. is a founder of Seromyx Systems, a company developing a platform technology that  
284 describes the antibody immune response. G.A.'s interests were reviewed and are managed by  
285 Massachusetts General Hospital and Partners HealthCare in accordance with their conflict of  
286 interest policies. All other authors have declared that no conflicts of interest exist.

287

288

## 289 **Methods**

### 290 Cohort

291 Pediatric vaccinee samples were obtained from children who were vaccinated with two doses  
292 100 µg mRNA-1273 at MGH as participants in Part 1 (open label) of a Phase2/3 clinical trial  
293 (ClinicalTrials.gov Identifier: NCT04796896). Additionally, we included samples from eight  
294 children who presented with acute PCR confirmed COVID-19 (7-19 years) or six children with  
295 MIS-C (3-22 years) at our hospital. Additionally, samples from 14 adults who received two  
296 doses mRNA-1273 as part of a phase 1 clinical trial were used as controls (ClinicalTrials.gov  
297 Identifier: NCT04283461). All pediatric participants provided informed assent and their legal  
298 guardian provided informed consent prior to participation in the MGH Pediatric COVID-19  
299 Biorepository. Blood samples and symptom report via an IRB-approved symptom questionnaire  
300 were collected prior to vaccination, one month after the first vaccination and one month after the  
301 second vaccination. This study was overseen and approved by the MassGeneral Institutional  
302 Review Board (IRB #2020P00955).

### 303 Antigens and biotinylation

304 All antigens were biotinylated using an NHS-Sulfo-LC-LC kit according to the manufacturer's  
305 instruction (Thermo Fisher, MA, USA) if required by the assay and excessive biotin was removed  
306 by size exclusion chromatography using Zeba-Spin desalting columns (7kDa cutoff, Thermo  
307 Fisher).

### 308 Antibody isotype and Fc receptor binding

309 Antigen-specific antibody isotype and subclass titers and Fc receptor binding profiles were  
310 analyzed with a custom multiplex Luminex assay as described previously (45). In brief, antigens

311 were coupled directly to Luminex microspheres (Luminex Corp, TX, USA). Coupled beads were  
312 incubated with diluted plasma samples washed, and Ig isotypes or subclasses with a 1:100  
313 diluted PE-conjugated secondary antibody for IgG1 (clone: HP6001), IgG2 (clone: 31-7-4), IgG3  
314 (clone: HP6050), IgG4 (clone: HP6025), IgM (clone: SA-DA4), IgA1 (clone: B3506B4) or IgA2  
315 (clone: A9604D2) (all Southern Biotech, AL, USA), respectively. For the Fc $\gamma$ R binding, a  
316 respective PE-streptavidin (Agilent Technologies) coupled recombinant and biotinylated human  
317 Fc $\gamma$ R protein was used as a secondary probe. Excessive secondary reagent was washed away  
318 after 1h incubation, and the relative antigen-specific antibody levels were determined on an iQue  
319 analyzer (Intellicyt).

#### 320 Antibody-Dependent Complement Deposition (ADCD)

321 Complement deposition was performed as described before(46). In brief, biotinylated antigens  
322 were coupled to FluoSphere NeutrAvidin beads (Thermo Fisher) and to form immune-complexes  
323 incubated with 10  $\mu$ l 1:10 diluted plasma samples for 2h at 37°C. After non-specific antibodies  
324 were washed away, immune-complexes were incubated with guinea pig complement in GVB++  
325 buffer (Boston BioProducts, MA, USA) for 20 min at 37°C. EDTA containing PBS (15mM) was  
326 used to stop the complement reaction and deposited C3 on beads was stained with anti-guinea pig  
327 C3-FITC antibody (MP Biomedicals, CA, USA, 1:100, polyclonal) and analyzed on an iQue  
328 analyzer (Intellicyt).

#### 329 Antibody-Dependent-Neutrophil-Phagocytosis (ADNP)

330 Phagocytosis score of primary human neutrophils was determined as described before(47).  
331 Biotinylated antigens were coupled to FluoSphere NeutrAvidin beads (Thermo Fisher) and  
332 incubated with 10  $\mu$ l 1:100 diluted plasma for 2h at 37°C to form immune-complexes. Primary

333 neutrophils were derived from Ammonium-Chloride-Potassium (ACK) buffer lysed whole blood  
334 from healthy donors and incubated with washed immune complexes for 1h at 37°C. Afterwards,  
335 neutrophils were stained for surface CD66b (Biolegend, CA, USA; 1:100, clone: G10F5)  
336 expression, fixed with 4% para-formaldehyde and analyzed on a iQue analyzer (Intellicyt).

#### 337 Antibody-Dependent-THP-1 Cell-Phagocytosis (ADCP)

338 THP-1 phagocytosis assay was performed as described before(48). In brief, biotinylated antigens  
339 were coupled to FluoSphere NeutrAvidin beads (Thermo Fisher) and incubated with 10 µl 1:100  
340 diluted plasma for 2h at 37°C to form immune complexes. THP-1 monocytes were added to the  
341 beads, incubated for 16 h at 37°C, fixed with 4% para-formaldehyde and analyzed on a iQue  
342 analyzer (Intellicyt).

#### 343 Antibody-Dependent-NK-Activation (ADNKA)

344 To determine Antibody-dependent NK cell activation, MaxiSporp ELISA plates (Thermo Fisher)  
345 were coated with respective antigen for 2h at RT and then blocked with 5% BSA (Sigma-Aldrich).  
346 50 µl 1:50 diluted plasma sample or monoclonal Abs was added to the wells and incubated  
347 overnight at 4°C. NK cells were isolated from buffy coats from healthy donors using the  
348 RosetteSep NK cell enrichment kit (STEMCELL Technologies, MA, USA) and stimulated with  
349 rhIL-15 (1ng/ml, STEMCELL Technologies) at 37°C overnight. NK cells were added to the  
350 washed ELISA plate and incubated together with anti-human CD107a (BD, 1:40, clone: H4A3),  
351 brefeldin A (Sigma-Aldrich, MO, USA), and monensin (BD) for 5 hours at 37°C. Next, cells were  
352 surface stained for CD56 (BD, 1:200, clone: B159), CD16 (BD, 1:200, clone: 3G8), and CD3 (BD,  
353 1:800, UCHT1). After fixation and permeabilization with FIX & PERM Cell Permeabilization Kit  
354 (Thermo Fisher), cells were stained for intracellular markers MIP1β (BD, 1:50, clone: D21-1351)



355 and IFN $\gamma$  (BD, 1:17, clone: B27). NK cells were defined as CD3-CD16+CD56+ and frequencies  
356 of degranulated (CD107a+), INF $\gamma$ + and MIP1 $\beta$ + NK cells determined on an iQue analyzer  
357 (Intellicyt)(49).

### 358 Virus neutralization

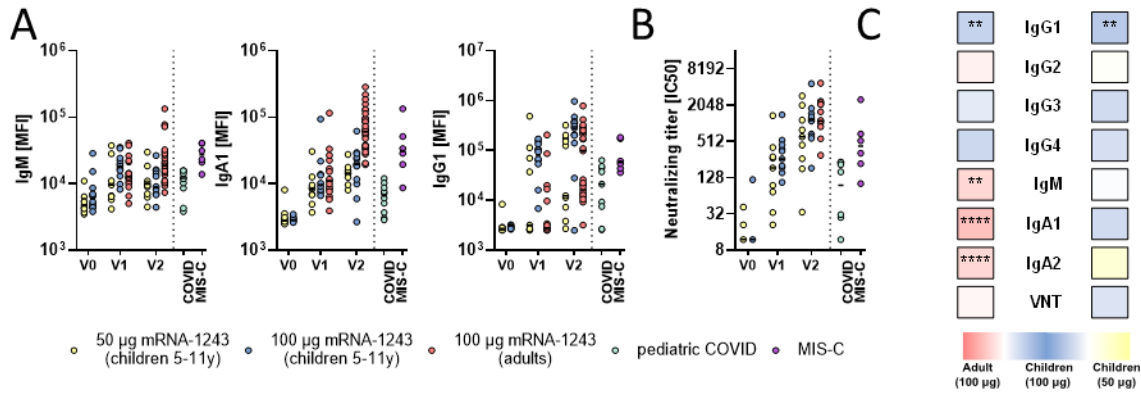
359 Three-fold serial dilutions ranging from 1:12 to 1:8748 were performed for each plasma sample  
360 before adding 50–250 infectious units of pseudovirus expressing the SARS-CoV-2 reference  
361 (Wuhan/wildtype) or delta variant Spike to hACE-2 expressing HEK293 cells for 1 hour.  
362 Percentage neutralization was determined by subtracting background luminescence measured in  
363 cell control wells (cells only) from sample wells and dividing by virus control wells (virus and  
364 cells only). Pseudovirus neutralization titers (pNT50) values were calculated by taking the inverse  
365 of the 50% inhibitory concentration value for all samples with a pseudovirus neutralization value  
366 of 80% or higher at the highest concentration of serum.

### 367 Data analysis and Statistics

368 Data analysis was performed using GraphPad Prism (v.9.2.0) and RStudio (v.1.3 and R v.4.0).  
369 Comparisons between the adults and children were performed using Wilcoxon-signed rank test  
370 followed by Benjamini-Hochberg (BH) correction. Multivariate classification models were built  
371 to discriminate humoral profiles between vaccination arms. Prior to analysis, all data were  
372 normalized using z-scoring. Feature selection was performed using least absolute shrinkage and  
373 selection operator (LASSO). Classification and visualization were performed using partial least  
374 square discriminant analysis (PLS-DA). Model accuracy was assessed using ten-fold cross-  
375 validation. These analyses were performed using R package “ropls” version 1.20.0 (50) and  
376 “glmnet” version 4.0.2(51). Co-correlates of LASSO selected features were calculated to find

377 features that can equally contribute to discriminating vaccination arms. Correlations were  
378 performed using Spearman method followed by Benjamini-Hochberg correction. The co-correlate  
379 network was generated using R package “network” version 1.16.0(52).

380

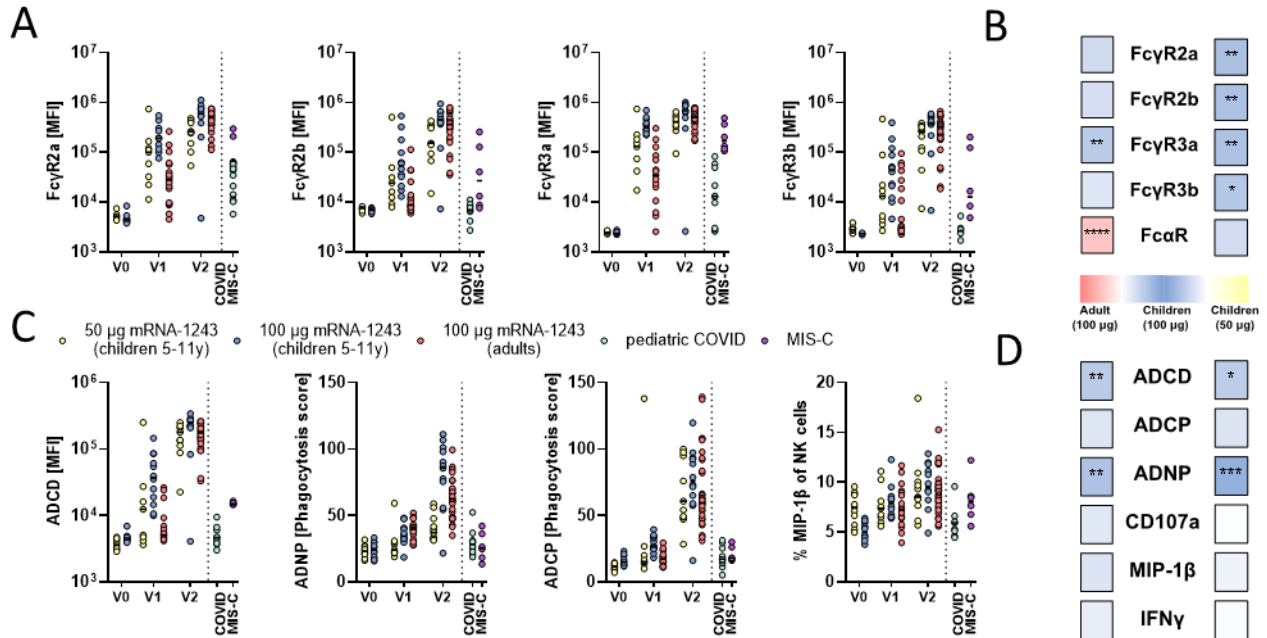


381

382 **Figure 1. mRNA-1273 vaccination induces robust binding and neutralizing titers in children**

383 A) Relative SARS-CoV-2 spike (Wuhan) specific IgM, IgA1 and IgG1 binding levels were  
 384 determined by Luminex in children (6-11 years) receiving 50µg or 100µg mRNA1273 before  
 385 (V0<sub>50</sub>: n=12; V0<sub>100</sub>: n=12), after the first (V1<sub>50</sub>: n=9; V1<sub>100</sub>: n=12) or after the second (V1<sub>50</sub>: n=11;  
 386 V2<sub>100</sub>: n=12) dose or in adults receiving two 100µg doses (V1: n=19; V2: n=33) as well as in  
 387 convalescent pediatric COVID (n=9) or MIS-C (n=6). B) The dot plots show the inverse 50 %  
 388 virus neutralizing titers in children (6-11 years) receiving 50µg or 100µg mRNA1273 before (V0<sub>50</sub>:  
 389 n=12; V0<sub>100</sub>: n=12), after the first (V1<sub>50</sub>: n=9; V1<sub>100</sub>: n=12) or after the second (V1<sub>50</sub>: n=9; V2<sub>100</sub>:  
 390 n=11) dose or in adults receiving two 100µg doses (V2: n=14) as well as in convalescent pediatric  
 391 COVID (n=9) or MIS-C (n=6). C) Heatmap strips summarize univariate comparison at the V2  
 392 timepoint of 100µg dose vaccinated children to adults (left panel) or to 50µg dose vaccinated  
 393 children (right panel). Color of the tiles indicate whether antibody binding titer were upregulated  
 394 in the respective group: 100µg vaccinated children (blue shades), adults (red shades), or 50µg  
 395 vaccinated children (yellow shades). A Wilcoxon-rank test was used to test for statistical  
 396 significance and asterisks indicate statistically significant differences of the respective feature after  
 397 Benjamini-Hochberg correction for multiple testing (\*:p<0.05; \*\*:p<0.01;\*\*\*:p<0.001).

398



399

400 **Figure 2. mRNA-1273 vaccination induces higher FcγR binding and phagocytic activity in**

401 **children.** A) Binding of SARS-CoV-2 specific antibodies to FcγR2a, 2b, 3a, and 3b was

402 determined by Luminex in children (6-11 years) receiving 50µg or 100µg mRNA1273 before

403 (V0<sub>50</sub>: n=12; V0<sub>100</sub>: n=12), after the first (V1<sub>50</sub>: n=9; V1<sub>100</sub>: n=12) or after the second (V1<sub>50</sub>: n=11;

404 V2<sub>100</sub>: n=12) dose or in adults receiving two 100µg doses (V1: n=19; V2: n=33) as well as in

405 convalescent pediatric COVID (n=9) or MIS-C (n=6). C) Heatmap strips summarize univariate

406 comparison of Fc receptor binding at the V2 timepoint of 100µg dose vaccinated children to adults

407 (left panel) or to 50µg dose vaccinated children (right panel). Color of the tiles indicate whether

408 antibody binding titer were upregulated in the respective group: 100µg vaccinated children (blue

409 shades), adults (red shades), or 50µg vaccinated children (yellow shades). C) The ability of SARS-

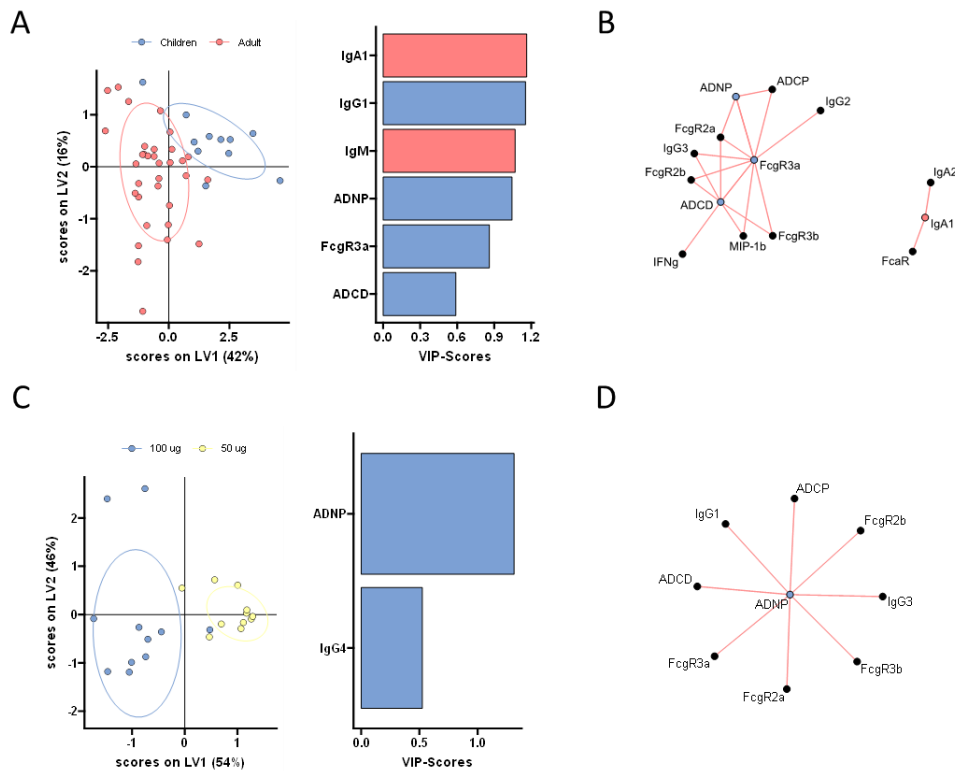
410 CoV-2 S specific antibody Fc to induce antibody-dependent-complement-deposition (ADCC),

411 neutrophil-phagocytosis (ADNP), cellular-THP1 monocyte-phagocytosis (ADCP), or activation

412 of NK cells marked by expression of MIP-1β was analyzed. D) Heatmap strips summarize

413 univariate comparison of Fc effector functions at the V2 timepoint of 100 $\mu$ g dose vaccinated  
414 children to adults (left panel) or to 50 $\mu$ g dose vaccinated children (right panel) as in B). A  
415 Wilcoxon-rank test was used to test for statistical significance in C) and D) and asterisks indicate  
416 statistically significant differences of the respective feature after Benjamini-Hochberg correction  
417 for multiple testing (\*:p<0.05; \*\*:p<0.01;\*\*\*:p<0.001).

418



419

420

421 **Figure 3. Distinct humoral profiles distinguish between adult and pediatric vaccine**

422 **responses.** A) A machine learning model was built using a minimal set of LASSO selected SARS-

423 CoV-2 S specific features at V2 (left panel) to discriminate between vaccine responses in adult

424 (red) and 100  $\mu$ g vaccinated children (purple) in a PLS-DA analysis (right panel). B) The co-

425 correlation network illustrates all LASSO-selected features. Nodes of selected features are colored

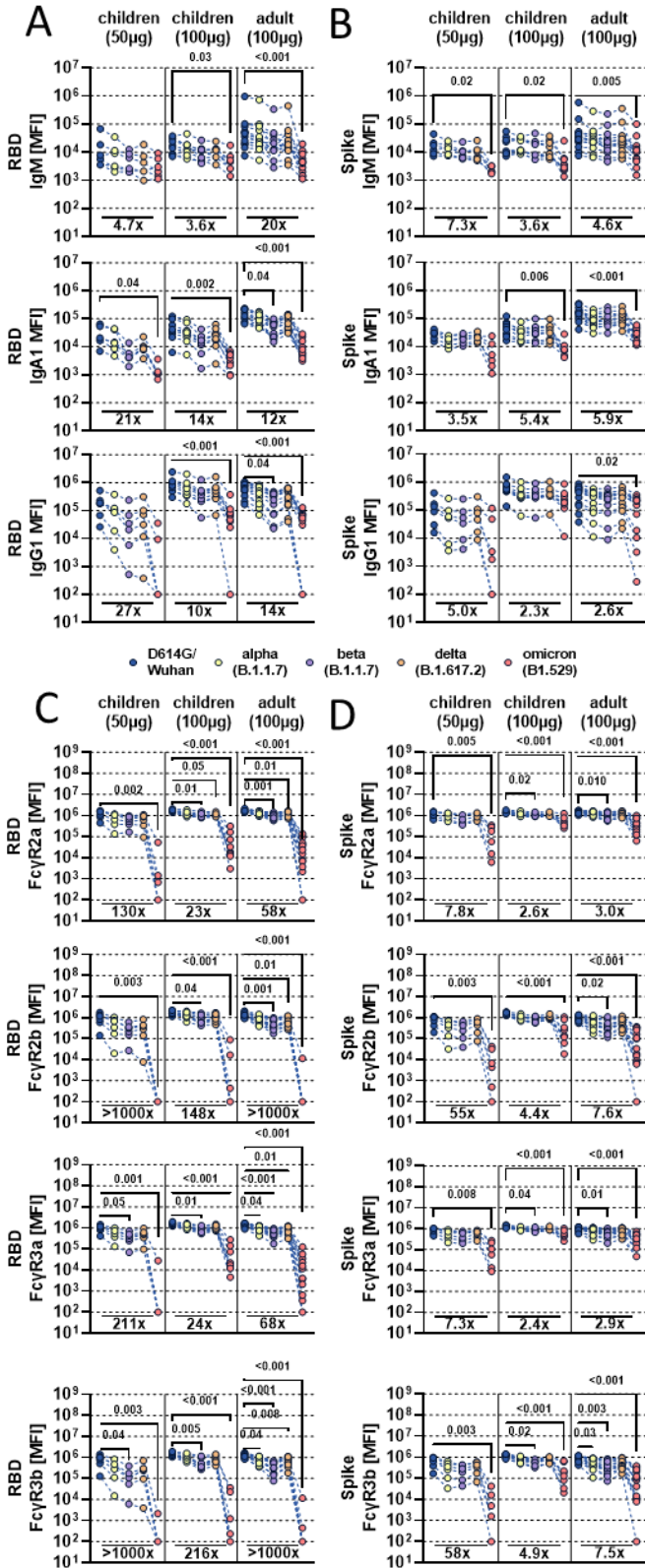
426 whether they were enriched in children (purple) or adults (red). Lines indicate significant ( $p < 0.05$ )

427 spearman correlations with  $|r| > 0.7$  of connected features (only positive correlations with  $r > 0$  were

428 observed). C) PLS-DA model of LASSO selected features at V2 (left panel) to discriminate

429 between vaccine responses in 100  $\mu$ g (purple) and 50  $\mu$ g (yellow) vaccinated children. D) The co-

430 correlation network as in B) illustrates all LASSO-selected features. Nodes of selected features are  
431 colored whether they were enriched in 100 µg vaccinated children (purple).





433 **Figure 4. mRNA-1273 vaccination elicits humoral responses to SARS-CoV-2 variants of**  
434 **concern.** A-B) The line graphs show the vaccine induced IgM, IgA1 and IgG1 recognition to  
435 D614G (WT; blue), alpha (B.1.117; yellow), beta (B.1.351; purple), delta (B.1.617.2; orange), and  
436 omicron (B.1.529; red) variants of concern receptor binding domains (A) or full Spike (B) for  
437 children ( $n_{50\mu\text{g}}=6$ ,  $n_{100\mu\text{g}}=9$ ) or adults ( $n=14$ ) at V2, where each individuals' response is linked  
438 across VOC antigens. C-D) The line graphs show the Fc $\gamma$ R (Fc $\gamma$ R2a, Fc $\gamma$ R2b, Fc $\gamma$ R3a, Fc $\gamma$ R3b)  
439 binding profiles of vaccine induced antibodies to RBD or Spike VOC antigens across children  
440 ( $n_{50\mu\text{g}}=6$ ,  $n_{100\mu\text{g}}=9$ ) or adults ( $n=12$ ) at V2, where each individuals' response is linked across VOC  
441 antigens. Background corrected data is shown and negative values were set to 100 for graphing  
442 purposes in A-D. A Kruskal-Wallis test with a Benjamini-Hochberg post-test correction for  
443 multiple comparisons was used to test for statistical differences between wildtype and VOC titers  
444 within groups. P-values for significantly different features are shown above and fold change  
445 reduction of omicron titer compared to wildtype below each dataset.

446

447

448

449

450

451

452

453

454 **Reference**

- 455 1. G. Matias *et al.*, Estimates of hospitalization attributable to influenza and RSV in the US  
456 during 1997-2009, by age and risk status. *BMC Public Health* **17**, 271 (2017).
- 457 2. J. F. Ludvigsson, Systematic review of COVID-19 in children shows milder cases and a  
458 better prognosis than adults. *Acta Paediatr* **109**, 1088-1095 (2020).
- 459 3. D. A. Siegel *et al.*, Trends in COVID-19 Cases, Emergency Department Visits, and  
460 Hospital Admissions Among Children and Adolescents Aged 0-17 Years - United States,  
461 August 2020-August 2021. *MMWR Morb Mortal Wkly Rep* **70**, 1249-1254 (2021).
- 462 4. CDC.gov, CenterForDiseaseControlAndPrevention.
- 463 5. M. J. Delahoy *et al.*, Hospitalizations Associated with COVID-19 Among Children and  
464 Adolescents - COVID-NET, 14 States, March 1, 2020-August 14, 2021. *MMWR Morb*  
465 *Mortal Wkly Rep* **70**, 1255-1260 (2021).
- 466 6. L. R. Feldstein *et al.*, Multisystem Inflammatory Syndrome in U.S. Children and  
467 Adolescents. *N Engl J Med* **383**, 334-346 (2020).
- 468 7. E. J. Schatorje, G. J. Driessen, R. W. van Hout, M. van der Burg, E. de Vries, Levels of  
469 somatic hypermutations in B cell receptors increase during childhood. *Clin Exp Immunol*  
470 **178**, 394-398 (2014).
- 471 8. Z. A. Bhutta, R. E. Black, Global maternal, newborn, and child health--so near and yet so  
472 far. *N Engl J Med* **369**, 2226-2235 (2013).
- 473 9. J. Bonhoeffer, C. A. Siegrist, P. T. Heath, Immunisation of premature infants. *Arch Dis*  
474 *Child* **91**, 929-935 (2006).
- 475 10. L. A. Jackson *et al.*, An mRNA Vaccine against SARS-CoV-2 - Preliminary Report. *N*  
476 *Engl J Med* **383**, 1920-1931 (2020).

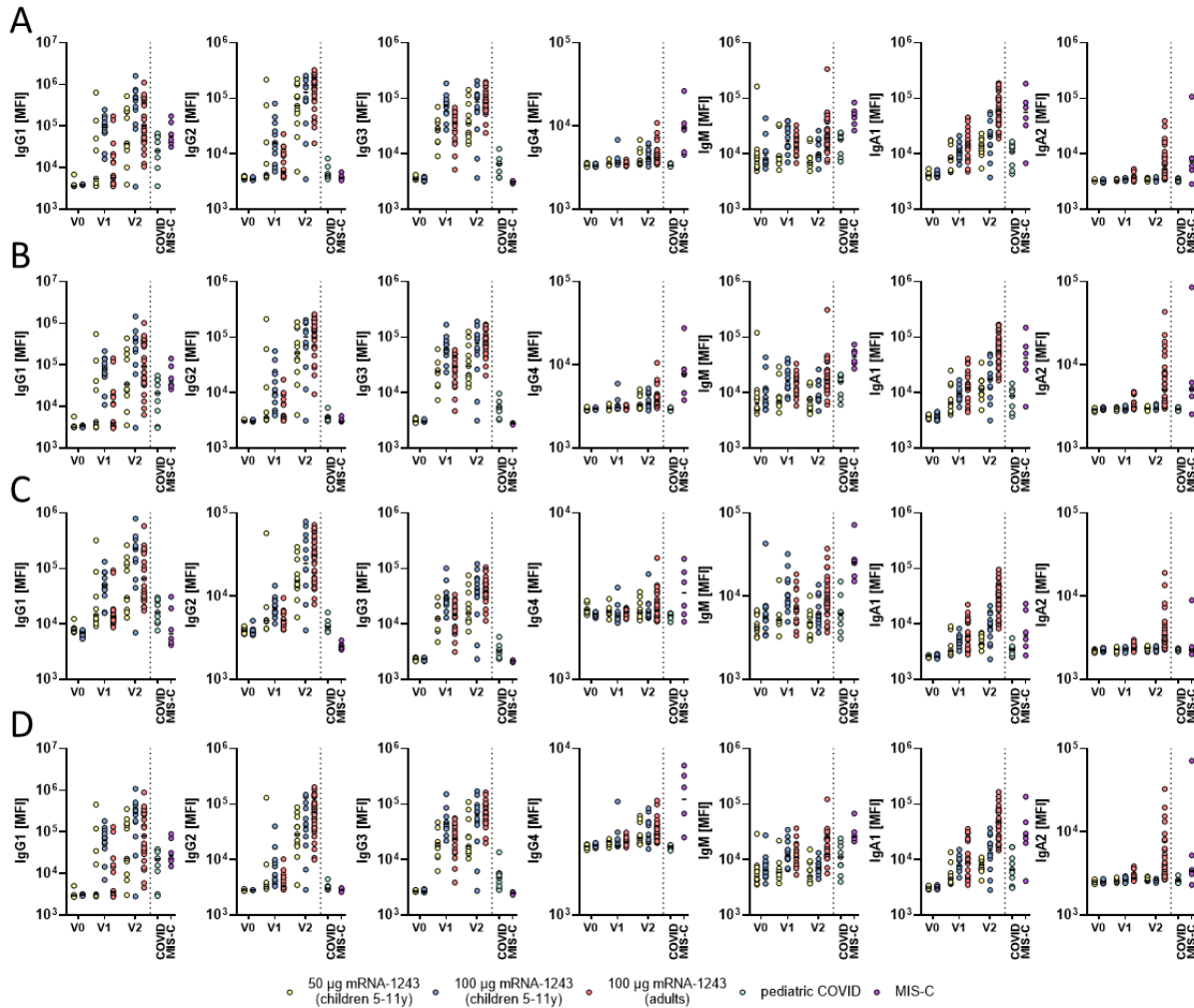
- 477 11. Press Release Pfizer Inc and BioNTech SE PFIZER AND BIONTECH PROVIDE  
478 UPDATE ON ONGOING STUDIES OF COVID-19 VACCINE. (2021).
- 479 12. T. Zohar *et al.*, Compromised Humoral Functional Evolution Tracks with SARS-CoV-2  
480 Mortality. *Cell* **183**, 1508-1519 e1512 (2020).
- 481 13. C. E. Z. Chan *et al.*, The Fc-mediated effector functions of a potent SARS-CoV-2  
482 neutralizing antibody, SC31, isolated from an early convalescent COVID-19 patient, are  
483 essential for the optimal therapeutic efficacy of the antibody. *PLoS One* **16**, e0253487  
484 (2021).
- 485 14. M. J. Gorman *et al.*, Fab and Fc contribute to maximal protection against SARS-CoV-2  
486 following NVX-CoV2373 subunit vaccine with Matrix-M vaccination. *Cell Rep Med*,  
487 100405 (2021).
- 488 15. T. Andrews, K. E. Sullivan, Infections in patients with inherited defects in phagocytic  
489 function. *Clin Microbiol Rev* **16**, 597-621 (2003).
- 490 16. D. N. Forthal, C. Moog, Fc receptor-mediated antiviral antibodies. *Curr Opin HIV AIDS*  
491 **4**, 388-393 (2009).
- 492 17. S. Chakraborty *et al.*, Proinflammatory IgG Fc structures in patients with severe COVID-  
493 19. *Nat Immunol* **22**, 67-73 (2021).
- 494 18. E. R. Stiehm, H. H. Fudenberg, Serum levels of immune globulins in health and disease: a  
495 survey. *Pediatrics* **37**, 715-727 (1966).
- 496 19. J. M. Woof, M. A. Kerr, IgA function--variations on a theme. *Immunology* **113**, 175-177  
497 (2004).
- 498 20. E. J. Haas *et al.*, Impact and effectiveness of mRNA BNT162b2 vaccine against SARS-  
499 CoV-2 infections and COVID-19 cases, hospitalisations, and deaths following a

- 500 nationwide vaccination campaign in Israel: an observational study using national  
501 surveillance data. *Lancet* **397**, 1819-1829 (2021).
- 502 21. J. S. Tregoning, K. E. Flight, S. L. Higham, Z. Wang, B. F. Pierce, Progress of the COVID-  
503 19 vaccine effort: viruses, vaccines and variants versus efficacy, effectiveness and escape.  
504 *Nat Rev Immunol* **21**, 626-636 (2021).
- 505 22. L. J. Abu-Raddad, H. Chemaitelly, A. A. Butt, C.-V. National Study Group for,  
506 Effectiveness of the BNT162b2 Covid-19 Vaccine against the B.1.1.7 and B.1.351  
507 Variants. *N Engl J Med* **385**, 187-189 (2021).
- 508 23. L. A. VanBlargan *et al.*, An infectious SARS-CoV-2 B.1.1.529 Omicron virus escapes  
509 neutralization by several therapeutic monoclonal antibodies. *bioRxiv*,  
510 2021.2012.2015.472828 (2021).
- 511 24. D. Planas *et al.*, Considerable escape of SARS-CoV-2 variant Omicron to antibody  
512 neutralization. *bioRxiv*, 2021.2012.2014.472630 (2021).
- 513 25. P. Kaplonek *et al.*, Subtle immunological differences in mRNA-1273 and BNT162b2  
514 COVID-19 vaccine induced Fc-functional profiles. *bioRxiv*, (2021).
- 515 26. L. R. Baden *et al.*, Efficacy and Safety of the mRNA-1273 SARS-CoV-2 Vaccine. *N Engl*  
516 *J Med* **384**, 403-416 (2021).
- 517 27. F. P. Polack *et al.*, Safety and Efficacy of the BNT162b2 mRNA Covid-19 Vaccine. *N*  
518 *Engl J Med* **383**, 2603-2615 (2020).
- 519 28. V. T. Chu *et al.*, Household Transmission of SARS-CoV-2 from Children and Adolescents.  
520 *N Engl J Med* **385**, 954-956 (2021).

- 521 29. L. M. Yonker *et al.*, Pediatric Severe Acute Respiratory Syndrome Coronavirus 2 (SARS-  
522 CoV-2): Clinical Presentation, Infectivity, and Immune Responses. *J Pediatr* **227**, 45-52  
523 e45 (2020).
- 524 30. L. M. Yonker *et al.*, Virologic features of SARS-CoV-2 infection in children. *J Infect Dis*,  
525 (2021).
- 526 31. C. B., H. M., "Children and COVID-19: State Data Report A joint report from the  
527 American Academy of Pediatrics and the Children's Hospital Association," (American  
528 Academy of Pediatrics and Children's Hospital Association,  
529 [https://downloads.aap.org/AAP/PDF/AAP%20and%20CHA%20-  
530 %20Children%20and%20COVID-  
531 19%20State%20Data%20Report%2012.23%20FINAL.pdf](https://downloads.aap.org/AAP/PDF/AAP%20and%20CHA%20-%20Children%20and%20COVID-19%20State%20Data%20Report%2012.23%20FINAL.pdf), 2021).
- 532 32. R. W. Frenck, Jr. *et al.*, Safety, Immunogenicity, and Efficacy of the BNT162b2 Covid-19  
533 Vaccine in Adolescents. *N Engl J Med* **385**, 239-250 (2021).
- 534 33. K. Ali *et al.*, Evaluation of mRNA-1273 SARS-CoV-2 Vaccine in Adolescents. *N Engl J*  
535 *Med*, (2021).
- 536 34. K. Wu *et al.*, Serum Neutralizing Activity Elicited by mRNA-1273 Vaccine. *N Engl J Med*  
537 **384**, 1468-1470 (2021).
- 538 35. K. McMahan *et al.*, Correlates of protection against SARS-CoV-2 in rhesus macaques.  
539 *Nature* **590**, 630-634 (2021).
- 540 36. J. R. Francica *et al.*, Protective antibodies elicited by SARS-CoV-2 spike protein  
541 vaccination are boosted in the lung after challenge in nonhuman primates. *Sci Transl Med*  
542 **13**, (2021).

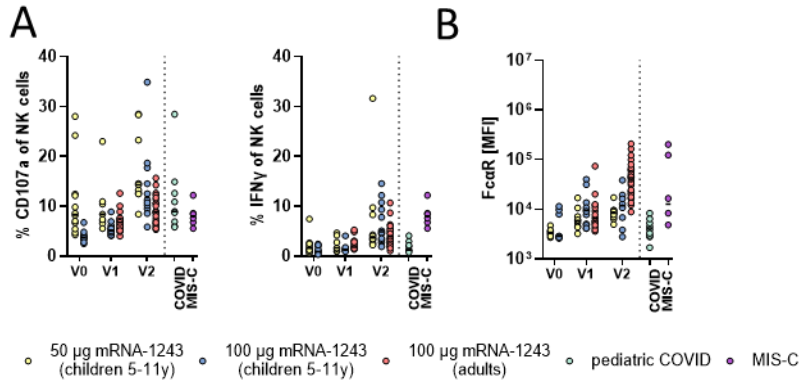
- 543 37. G. Alter, T. H. M. Ottenhoff, S. A. Joosten, Antibody glycosylation in inflammation,  
544 disease and vaccination. *Semin Immunol* **39**, 102-110 (2018).
- 545 38. A. K. Simon, G. A. Hollander, A. McMichael, Evolution of the immune system in humans  
546 from infancy to old age. *Proc Biol Sci* **282**, 20143085 (2015).
- 547 39. A. Vatti *et al.*, Original antigenic sin: A comprehensive review. *J Autoimmun* **83**, 12-21  
548 (2017).
- 549 40. J. J. Goronzy, C. M. Weyand, T cell development and receptor diversity during aging. *Curr*  
550 *Opin Immunol* **17**, 468-475 (2005).
- 551 41. L. Garderet *et al.*, The umbilical cord blood alphabeta T-cell repertoire: characteristics of  
552 a polyclonal and naive but completely formed repertoire. *Blood* **91**, 340-346 (1998).
- 553 42. P. Elliott *et al.*, Rapid increase in Omicron infections in England during December 2021:  
554 REACT-1 study. *medRxiv*, 2021.2012.2022.21268252 (2021).
- 555 43. I. M. Osmanov *et al.*, Risk factors for long covid in previously hospitalised children using  
556 the ISARIC Global follow-up protocol: A prospective cohort study. *Eur Respir J*, (2021).
- 557 44. A. B. Payne *et al.*, Incidence of Multisystem Inflammatory Syndrome in Children Among  
558 US Persons Infected With SARS-CoV-2. *JAMA Netw Open* **4**, e2116420 (2021).
- 559 45. E. P. Brown *et al.*, High-throughput, multiplexed IgG subclassing of antigen-specific  
560 antibodies from clinical samples. *J Immunol Methods* **386**, 117-123 (2012).
- 561 46. S. Fischinger *et al.*, A high-throughput, bead-based, antigen-specific assay to assess the  
562 ability of antibodies to induce complement activation. *J Immunol Methods* **473**, 112630  
563 (2019).
- 564 47. C. B. Karsten *et al.*, A versatile high-throughput assay to characterize antibody-mediated  
565 neutrophil phagocytosis. *J Immunol Methods* **471**, 46-56 (2019).

- 566 48. M. E. Ackerman *et al.*, A robust, high-throughput assay to determine the phagocytic  
567 activity of clinical antibody samples. *Journal of immunological methods* **366**, 8-19 (2011).
- 568 49. L. L. Lu *et al.*, A Functional Role for Antibodies in Tuberculosis. *Cell* **167**, 433-443 e414  
569 (2016).
- 570 50. E. A. Thevenot, A. Roux, Y. Xu, E. Ezan, C. Junot, Analysis of the Human Adult Urinary  
571 Metabolome Variations with Age, Body Mass Index, and Gender by Implementing a  
572 Comprehensive Workflow for Univariate and OPLS Statistical Analyses. *J Proteome Res*  
573 **14**, 3322-3335 (2015).
- 574 51. J. H. Friedman, T. Hastie, R. Tibshirani, Regularization Paths for Generalized Linear  
575 Models via Coordinate Descent. *2010* **33**, 22 (2010).
- 576 52. C. T. Butts, network: a Package for Managing Relational Data in R. *Journal of Statistical*  
577 *Software* **24**, (2008).



579 **Supplemental Figure 1. Vaccine induced antibody responses to different SARS-CoV-2**  
580 **variants of concern. IgG subclass (IgG1, IgG2, IgG3, IgG4) and isotype (IgM, IgA1, IgA2) titers**  
581 **are shown to the receptor binding domain of wildtype (A), alpha (B), beta (C), and delta (D)**  
582 **variants of concern.**





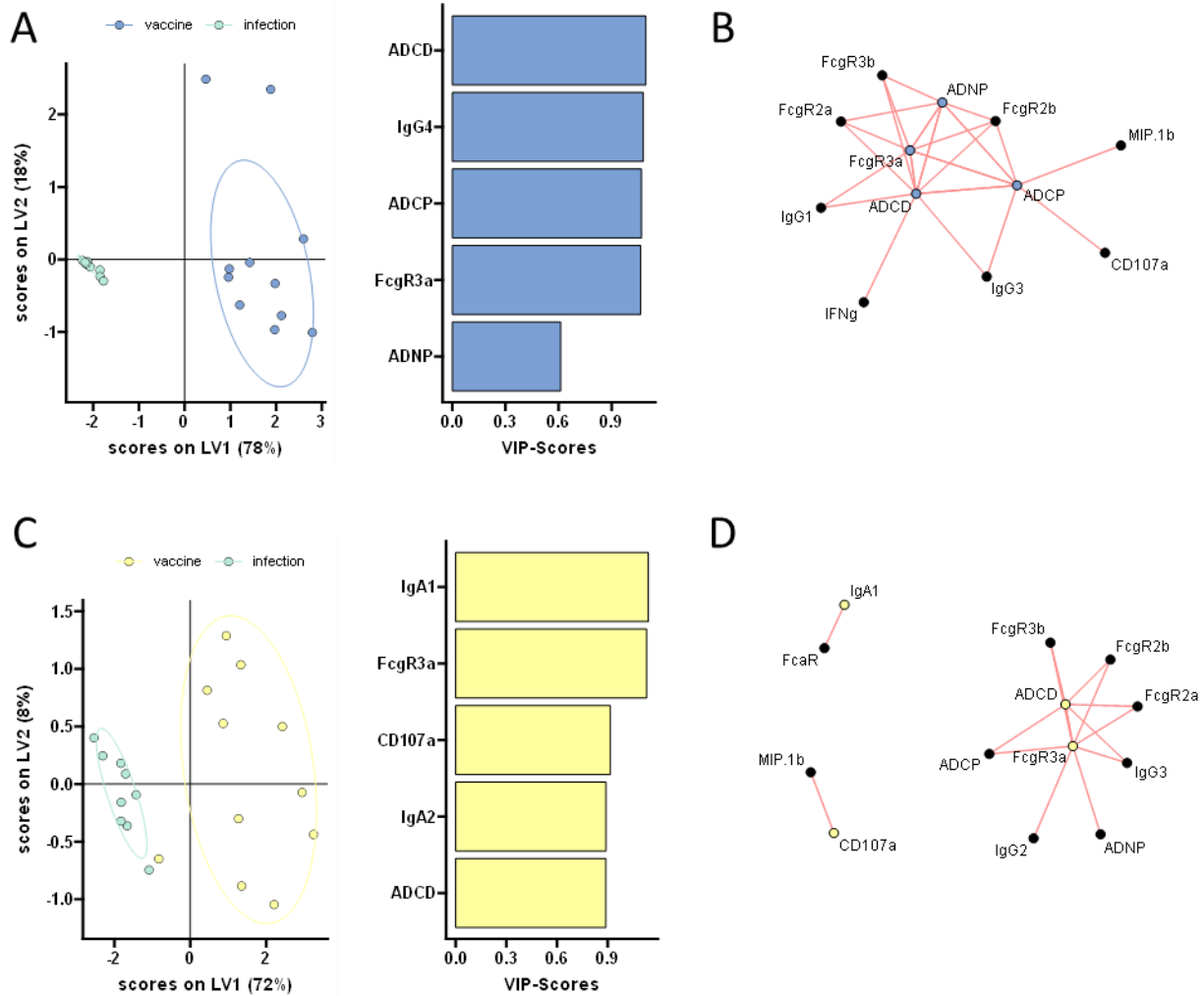
583

584 **Supplemental Figure 2. Univariate comparisons across vaccine profiles in children and**

585 **adults.** A) The plots show the antibody dependent NK cell activating (ADNKA, CD107a and IFN

586  $\gamma$  expression) levels in children and adults to the SARS-CoV-2 wt spike. B) The plots show the

587 binding of SARS-CoV-2 wildtype specific IgA antibodies to Fc $\alpha$ R by Luminex.



588

589 **Supplemental Figure 3. Distinct humoral profiles in naturally infected and vaccinated**

590 **children.** A machine learning model was built to compare SARS-CoV-2 profiles in naturally

591 infected and 100  $\mu$ g (A) or 50  $\mu$ g (C) vaccinated children. A minimal set of LASSO selected

592 SARS-CoV-2 S specific features (left panel) were first selected and used to discriminate pediatric

593 vaccine responses (at V2) from natural infection (acute COVID) in children. Only five features

594 were sufficient to completely separate the two groups. A co-correlate network was used to define  
595 additional features that differed in infection 100  $\mu$ g (B) or 50  $\mu$ g (D) vaccinated in children.

596